The rheology of fibre spinning and the properties of hollow-fibre membranes for gas separation

S. J. Shilton* and G. Bell
Department of Chemical and Process Engineering, University of Strathclyde, James Weir Building, 75 Montrose Street, Glasgow G1 1XJ, UK

and J. Ferguson
Department of Pure and Applied Chemistry, University of Strathclyde, Thomas Graham Building, 295 Cathedral Street, Glasgow G1 1XL, UK
(Received 14 February 1994; revised 3 May 1994)

The effect of spinning rheology on gas-separation hollow-fibre membranes has been investigated. For polysulfone fibres, permeability decreased with increasing dope concentration. The lowest fibre selectivities occurred with the medium spinning-dope concentration, suggesting that both surface pore area and active layer thickness were high. Both permeability and selectivity increased with increasing dope extrusion rate, possibly due to enhanced orientation of the membrane skin. Permeability increased and selectivity decreased with increasing jet stretch. Polyacrylonitrile membranes, because of the low polymer permeability, proved insensitive to spinning conditions, showing no separation capability due to the dominating effect of surface pores.

(Keywords: spinning rheology; hollow-fibre membranes; gas separation)

INTRODUCTION

Hollow-fibre membranes are produced by the dry-jet wet-spinning process. This involves the extrusion of a more or less concentrated polymer solution through an annulus in which it is subjected to shear flow. The fluid then passes through an air gap in which the dominant mode of deformation is elongational. Simultaneously, the coagulant flowing through the centre of the liquid filament (*Figure 1*) starts to cause coagulation from the centre outwards. Next, the fluid passes into the coagulating bath, where the coagulation front passing from the outside inwards ultimately meets the other front, at which point coagulation is more or less complete. It should be noted that it is possible for the coagulating fluid to pass through a gel phase before solidification. Generally, however, for membrane purposes this is not desirable, and only rapid coagulation to form a skin on the outer and inner surfaces (an asymmetric fibre) will be considered. The consequences of the rapid coagulation are that the rheological properties of the spinning dope may well play an important role in determining the permeability and separation characteristics of the membrane. It could, for example, be anticipated that oriented polymeric molecules coagulating from a shear-thinning viscoelastic fluid would form an oriented membrane skin. Electron microscopic examination of sections of rapidly coagulated hollow-fibre membranes do show the existence of skinned walls. The question now is whether or not the skin is oriented and, if so, whether this could be due to the fluid rheology.

The work that has been published correlating spinning conditions with membrane performance focuses on coagulation conditions[1]. Owing to the complexity of the polymer precipitation process, such work inevitably tends to the empirical. The current work seeks to improve fundamental knowledge of the spinning of gas-separation hollow-fibre membranes by adopting a rheological perspective, investigating the effects of shear and elongation experienced in the spinning line. The effect of shear was examined by altering the dope extrusion rate (DER) from the spinneret, and the effect of elongation was examined by altering the jet stretch ratio (JS), i.e. the ratio of wind-up speed to extrusion speed. When investigating DER or JS, it is important to keep the other one constant, though previous studies have not done this[2,3].

Altering the rheological conditions during fibre spinning is known to affect the properties of textile fibres[4–7] and ultrafiltration hollow-fibre membranes[8] due to changes in polymer orientation.

EXPERIMENTAL

Polymers

Two polymers were used, polysulfone (PSF; Amoco Chemicals, Udel P1700, weight-average molecular weight 35400) and polyacrylonitrile (PAN) copolymer (Courtaulds, P82, a copolymer of acrylonitrile and methyl

* To whom correspondence should be addressed

0032-3861/94/24/5327–09

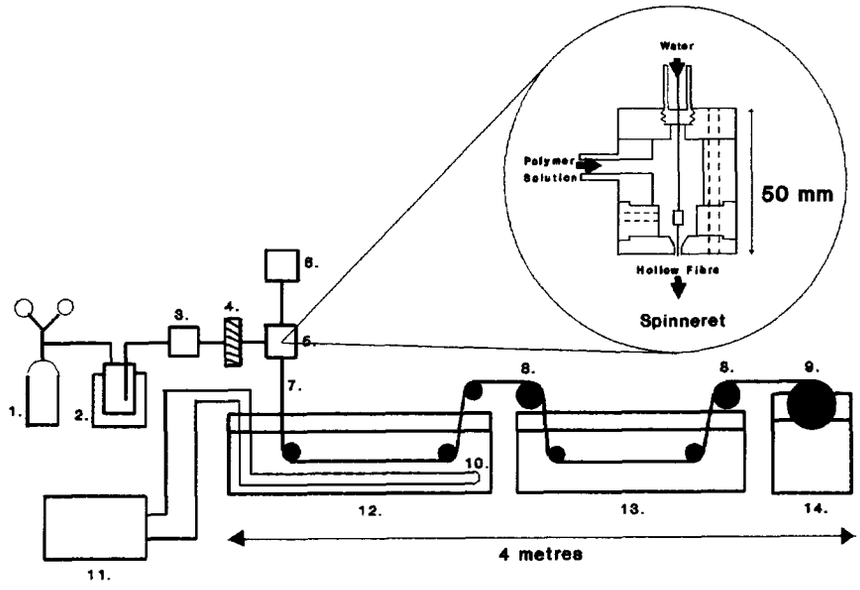

Figure 1 Hollow-fibre membrane spinning apparatus: (1) nitrogen; (2) dope reservoir; (3) gear pump; (4) filter, 7 μm; (5) spinneret; (6) water pump; (7) hollow fibre; (8) motor-driven roller, $D = 8$ cm; (9) motor-driven wind-up roller, $D = 16$ cm; (10) heat transfer coil; (11) refrigeration/heating unit; (12) coagulation bath, $L = 160$ cm; (13) washing/treatment bath, $L = 140$ cm; (14) wind-up bath

methacrylate containing approximately 15% methyl methacrylate, weight-average molecular weight 107 500). The solvent used to prepare the spinning solutions was dimethylformamide (DMF).

Spinning solution rheology

Shear flow was measured at 20°C using a Carri-Med Controlled Stress Rheometer with parallel-plate geometry. Each polymer solution was subjected to a range of shear rates covering those encountered in flow through the spinneret. The shear rates experienced in the spinneret were estimated by using the zero-shear viscosity derived from creep tests, assuming Newtonian behaviour and solving the flow equations for flow in a concentric annulus. The shear rate was found to be in the region of 10^4 s^{-1}. To achieve this, a 1 cm plate was used with a gap of 16 to 20 μm, depending on the exact shear-rate range and the solution under examination.

Each example was subjected to incrementally increasing shear stress, a period of constant shear and an incrementally decreasing shear stress. No evidence of thixotropy was found, since the up and down curves were identical. The viscosities calculated were, as a result, equilibrium values.

Creep tests using the same instrument were made to determine relaxation and retardation times. This involved subjecting the fluid to a small constant stress and measuring the variation of strain with time. Stress was then removed and the strain recovery followed as the fluid relaxed.

First normal stress difference, N_1, in shear is strongly related to the degree of elasticity of a fluid. Measurements of this parameter were made using an R16 Weissenberg Rheogoniometer with a 7.5 cm diameter cone and plate at 20°C.

A Carri-Med Elongational Viscometer as described by Ferguson and Hudson[9] was used for elongational flow measurements at 20°C. In order to obtain data over as wide a range of elongation rates as possible, extrusion rate, filament length and take-up velocity were all altered, and the resulting drawing force and filament dimensions recorded. Filament dimensions were recorded using a video camera attached to an Eltime Image III Analyser from Oxford Framestore Applications Ltd. Average values of tensile stress, strain rate and elongational viscosity were calculated using the technique described by Jackson *et al.*[10] and Jones *et al.*[11].

Membrane spinning

Polysulfone and PAN copolymer hollow-fibre membranes were produced from solutions in DMF using a dry-jet wet-spinning technique[8,12–14]. Membranes were spun under various conditions of shear and elongation and then characterized with respect to physical properties, morphology, gas permeability and selectivity.

Figure 1 shows the hollow-fibre spinning apparatus. The capillary-in-orifice spinneret was developed from a design suggested in a Monsanto patent[15]. The dope reservoir was immersed in a water bath for temperature control. The dope was fed to the spinneret via a gear pump. The reservoir was kept under nitrogen pressure (20 psig; ~138 kPa) as a precaution against cavitation in the line to the pump. The gear pump smoothly delivered polymer solution to the spinneret in the flow-rate range of 0.3–10 ml min^{-1}. An in-line filter (7 μm) prevented any extraneous material being passed to the spinneret from the gear pump. A ram and syringe type infusion pump provided an accurate and pulse-free supply of water to the capillary in the spinneret. The required water flow-rate range was 0.1–5 ml min^{-1}.

The dope passed through the spinneret and was extruded through the annular orifice. Water passed through the capillary section of the spinneret and was injected into the middle of the polymer solution as it was extruded, thus forming the basis of a hollow fibre. This incipient filament travelled through a 3.5 cm air gap before being passed via a series of rollers first through the coagulation bath and then the washing/treatment bath.

The speed of the fibre filament as it passed through the baths was controlled by the two 8 cm diameter motor-driven rollers. Lastly, the fully formed hollow fibre was wound up without overlap on the final wind-up drum. This drum had a diameter of 16 cm, and thus after a single traverse cut the fibres opened out to a suitable working length of 50 cm. The fibres were steeped in distilled water for 48 h to remove any residual solvent and hung vertically to dry for 72 h in a controlled-environment laboratory before being stored.

The temperature of the coagulation bath was controlled to within 0.1°C by a refrigeration/heating unit. The coagulant used throughout the experiments was water, both in the core (lumen) and in the coagulation baths. The core coagulant temperature was 20°C and that of the bath was 4°C. These coagulation conditions ensured rapid solidification when the spinning dope came in contact with coagulant.

The three key variables altered during the spinning runs were: spinning-dope concentration (C_D), dope extrusion rate (DER) and jet stretch ratio (JS). *Table 1* summarizes the general spinning conditions.

Membrane modules

Each membrane module comprised a bundle of 10 fibres of length 30 cm. The fibre bundle was potted at one end, in a tube sheet using polyurethane resin, in such a way as to leave the fibre lumens open. At the other end of the bundle, the fibres were sealed using a small end cap. The fibre module was then incorporated into the gas permeation apparatus (*Figure 2*).

Table 1 General hollow-fibre spinning conditions

Spinneret dimensions	0.600/0.330/0.178 mm
Dope temperature	25°C
N_2 blanket pressure	20 psig
Dry-jet height	3.5 cm
Dope extrusion rate:water injection rate	3:1
Lumen coagulant temperature	20°C
Coagulation bath temperature	4°C
Composition of coagulants	Pure water
Secondary stretching	None

Membrane coating

The fibres were coated with a highly permeable elastomeric silicone polymer[16]. The purpose of the coating was to fill any surface pinholes or imperfections, which render the fibres useless for gas separation. Blocking these cavities results in a decrease in permeability but improved selectivity. Coating may be regarded as a standard procedure that allows the hollow fibre to exhibit permeation properties closer to the inherent characteristics of the membrane polymer itself.

The coating was applied by dipping the fibre modules into solutions of silicone (polydimethylsiloxane, Dow Corning 200/1000cs) in hexane for 15 min and applying a slight vacuum to the lumen side. Two coating solution strengths were used: 3 wt% and 15 wt%. After coating, the modules were stored in a clean environment for a few days to allow curing.

The polysulfone fibres were coated with the 3 wt% silicone solution—using the 15 wt% solution had no further effect on the polysulfone membranes.

Permeability and selectivity tests

The gas permeability of the membranes was evaluated by fixing the fibre modules in a pressure chamber, pressurizing and then measuring the resulting gas transmission rate. The test gases used in this work were pure carbon dioxide and methane. The pressure difference across the membrane modules in the tests was 5 bar. An overall view of the gas permeation apparatus is shown in *Figure 2*. Permeability P is given by:

$$P = \frac{Q}{A\Delta p}$$

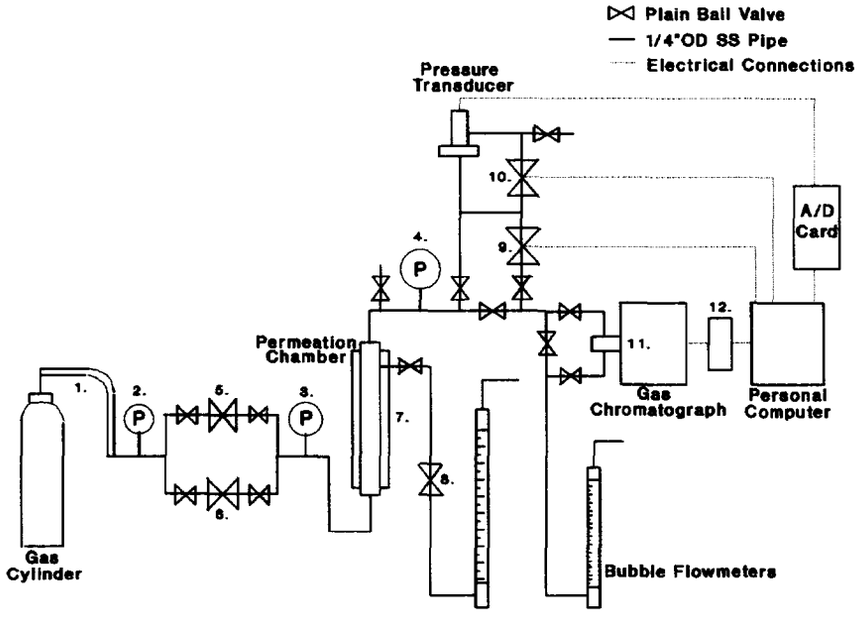

Figure 2 Hollow-fibre gas permeation apparatus: (1) flexible high-pressure host; (2) pressure gauge, 0–350 bar; (3) pressure gauge, 0–40 or 0–100 bar; (4) pressure gauge, 0–1 bar; (5) high-pressure regulator, delivery pressure = 35–240 bar; (6) low-pressure regulator, delivery pressure = 0–60 bar; (7) temperature-control water jacket; (8) needle valve; (9) solenoid valve no. 1; (10) solenoid valve no. 2; (11) automatic gas sampling valve; (12) GC/PC interface

where Q is flow rate, A is membrane surface area and Δp is pressure difierence. Membrane selectivity Ω with respect to any two gases, i and j, is the ratio of permeabilities:

$$\Omega_j^i = \frac{P_i}{P_j}$$

Dimensions and porosity

Fibre outer diameter was measured using digital callipers (confirmed using a light microscope with calibrated graduated view lens), and lumen diameters were determined from electron micrographs. Fibre void volume fraction was evaluated by comparing the bulk volume of the fibre to that of the solid polymer; the bulk volume being calculated from fibre dimensions and linear density (mass per unit length of fibre).

Tensile properties

Fibre behaviour under tensile stress has been standardized with respect to fibre linear density (units: g/km or tex) as opposed to cross-sectional area. In this way performance relates to the properties of the solid polymer within a fibre regardless of porosity.

An Instron 1122 Materials Testing Instrument was used to carry out the tensile tests. The trials were carried out in a controlled-environment laboratory (T = 20°C, r.h. = 65%) where the fibre samples were allowed to condition prior to testing. Results were based on the average of six tests for each fibre. A fibre gauge length of 40 mm was used throughout. A standard tensile test curve of specific stress (N/tex) against strain (extension/original length) was produced for each fibre. The main parameters of interest are as follows:

(i) Fibre strength, i.e. tenacity (N/tex)
= specific stress at break
= (load at break)/(linear density of fibre)
(ii) First tensile modulus, M_1 (N/tex)
= slope of stress–strain curve before yield point
= stress required per unit of strain before yield point
(iii) Second tensile modulus, M_2 (N/tex)
= slope of stress–strain curve after yield point
= stress required per unit of strain after yield point

M_1 is a measure of resistance to extension before the elastic limit is reached, and M_2 is a measure of resistance to extension after yield.

Fibre morphology by electron microscopy

Hollow-fibre samples 1–2 mm in length were cut using a fresh razor blade and mounted on sample stubs. These were then sputter coated with gold before being viewed with the electron microscope (Philips Scanning Electron Microscope model 500 or JEOL SEM model 840 A).

RHEOLOGICAL BEHAVIOUR

Shear-flow behaviour

Figures 3 and *4* show typical shear flow curves of the polymer solutions. Both polysulfone and PAN copolymer solutions exhibit shear-thinning behaviour in the spinning region, apart from the least concentrated polysulfone solution, which displayed the second Newtonian regime. The PAN copolymer solutions were more non-Newtonian at shear rates experienced in the spinneret.

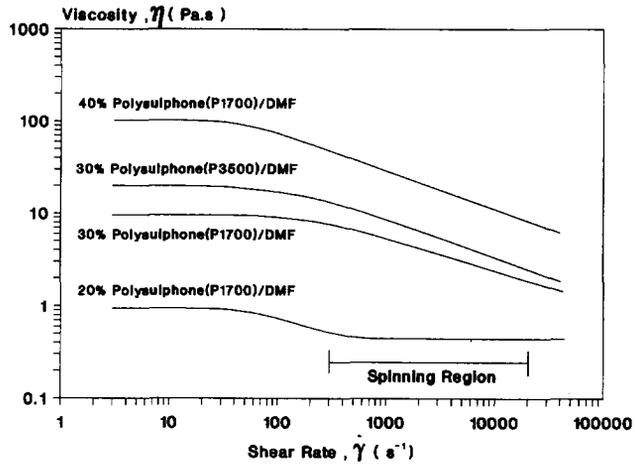

Figure 3 Behaviour of polysulfone dopes under shear

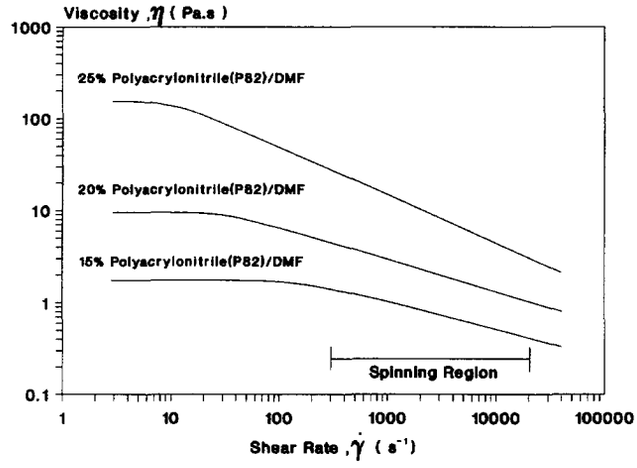

Figure 4 Behaviour of PAN copolymer dopes under shear

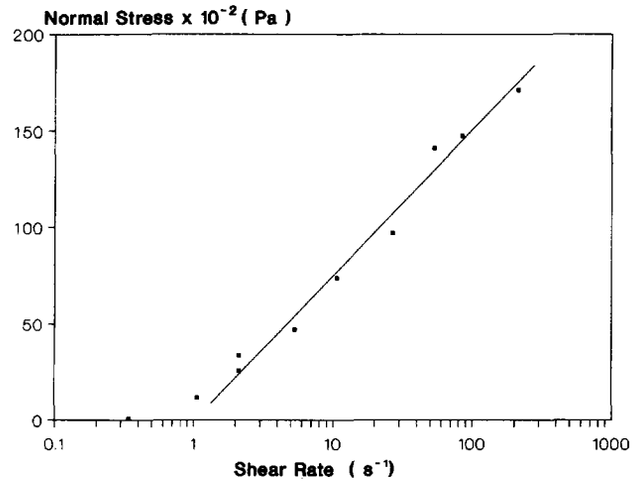

Figure 5 Normal stress of 25 wt% PAN copolymer in DMF

Only the most concentrated PAN copolymer solution (25 wt%) showed a measurable normal stress difference (*Figure 5*) and a detectable creep relaxation time (127 s, strain 0.36). Creep experiments represent essentially zero-shear conditions and relaxation times correspond to small levels of deformation.

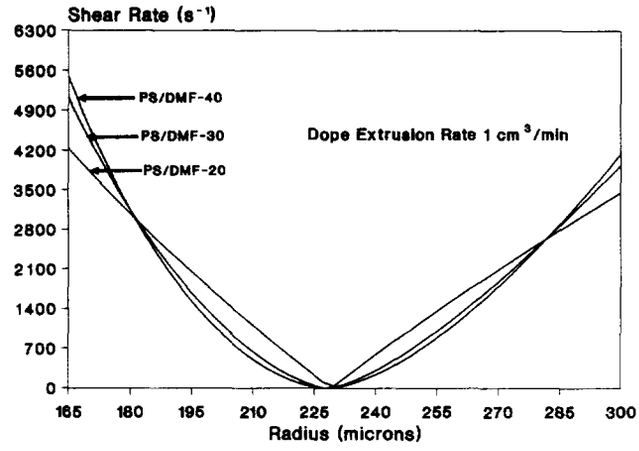

Figure 6 Shear-rate profiles in spinneret: polysulfone dopes

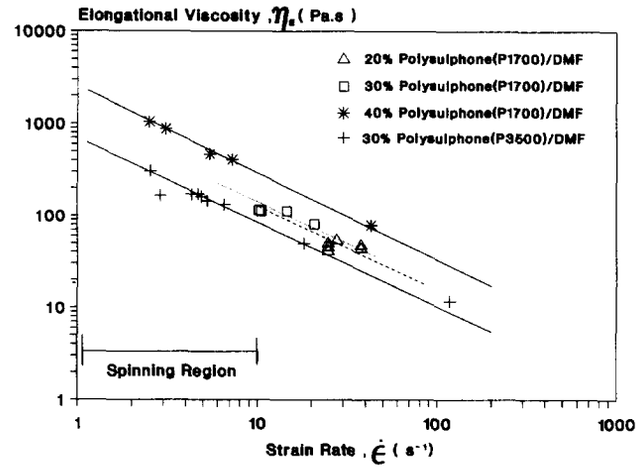

Figure 8 Behaviour of polysulfone dopes under elongation

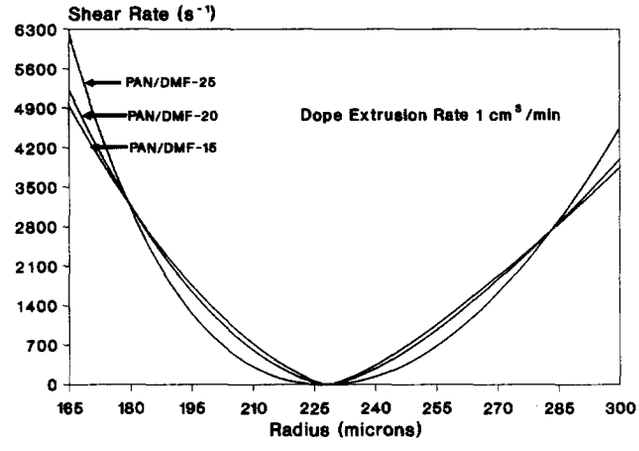

Figure 7 Shear-rate profiles in spinneret: PAN copolymer dopes

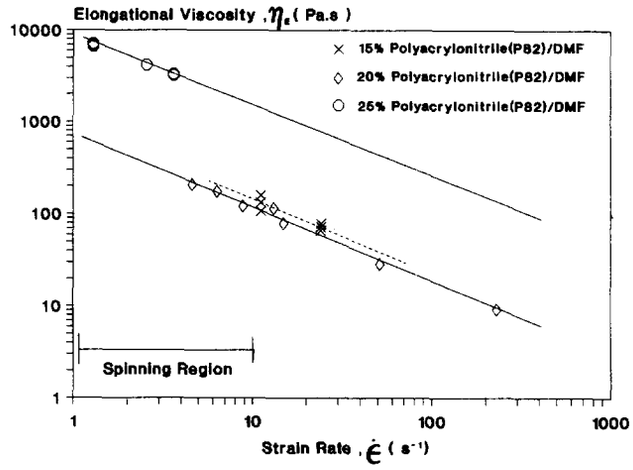

Figure 9 Behaviour of PAN copolymer dopes under elongation

Annular shear

Typical shear-rate profiles for the spinning dopes in the spinneret annulus are shown in *Figures 6* and *7*. These graphs were produced by solving the flow equations for a power-law fluid in a concentric annulus[17]. Note that the curves are skewed, with the higher shear rates being encountered at the inner surface of the annulus. This could have important consequences for the molecular orientation in the filament as it emerges from the spinneret. Since the shear rates are different at the inner and outer surfaces of the annulus, the distribution of first normal stress differences, N_1, where they exist, would be skewed also.

Extensional flow

Figures 8 and *9* show that the polymer solutions were strain-thinning over the strain rates tested including those encountered in spinning, i.e. when the filament is extended in the air gap between the spinneret and the coagulating bath. Lodge[18] has defined the conditions for stability (inherent spinnability) in a fluid as those in which extensional viscosity increases with strain rate. There is much evidence to support this view[19]. It is clear, therefore, that none of the spinning dopes is inherently spinnable. Imposition of too high a stretch rate would lead to failure of the liquid filament in the air gap. It would appear, therefore, that coagulation from the inner surface of the annulus formed by the polymer solutions as they emerge from the spinneret must play an important part in conferring stability (spinnability). The coagulation process invariably causes an increase in tensile modulus and in overall elongational viscosity[20].

Jones *et al.*[11] showed that the Trouton ratio (the ratio of shear viscosity η to elongational viscosity η_E) has a value of 3 for inelastic fluids, and that values higher than this indicate extent of viscoelasticity. Calculated Trouton ratios indicate that all polymer solutions were viscoelastic in the strain-rate range experienced during spinning[17].

The question now arises as to the significance of the rheological properties of the polymer solutions. The rate of extension in the air gap is relatively low (~ 1–$5\ s^{-1}$) and relaxation from the levels of shear experienced in the spinneret will be rapid (although the filament may retain some deformation at low levels of residual strain). It is probable, therefore, that when entering the coagulation bath the bulk of the filament will not be in a highly oriented state. However, conditions at the inner surface are quite different. Here coagulation occurs immediately the fluid leaves the spinneret and comes in contact with the water filling the lumen. Relaxation from shear will not have had time to occur and even the relatively small imposed extensional deformation will be 'frozen in'. These effects would be greater in the PAN copolymer filaments.

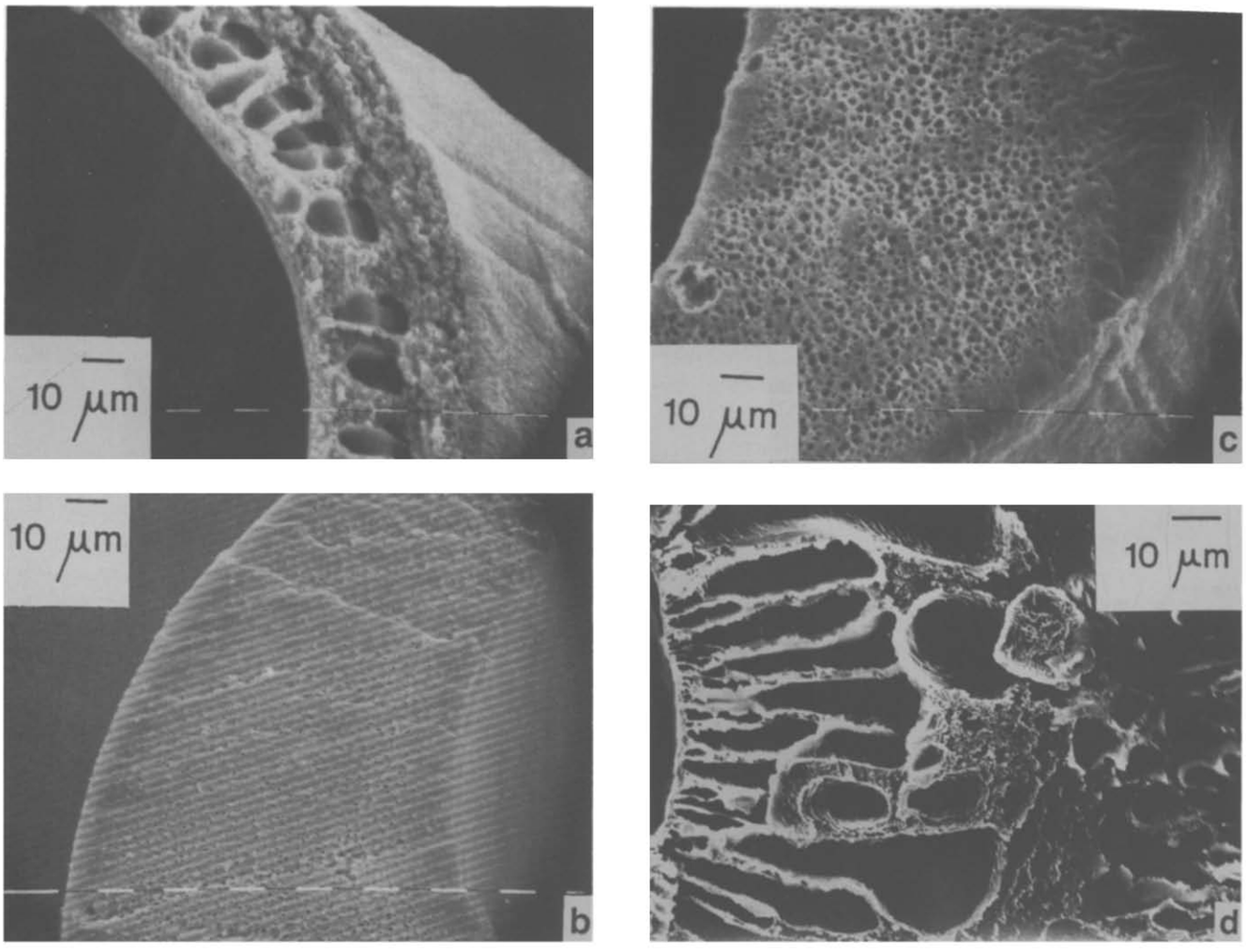

Figure 10 Cross-section of hollow fibres spun from various dope concentrations: (a) PSF 20 wt%; (b) PSF 30 wt%; (c) PSF 40 wt%; (d) PAN 25 wt%

POLYSULFONE MEMBRANES

This paper concentrates on polysulfone fibres because their gas permeation properties were more sensitive to spinning conditions. The results for PAN copolymer are confined to a separate section.

Morphology

No distinction in morphology, i.e. cross-sectional void structure and thickness of dense layer, was detected between the fibres spun at various levels of stretch and extrusion rate within any one particular dope concentration (the overall size of a fibre will obviously depend on the jet stretch ratio). The electron micrographs show the effect of polymer concentration in the spinning solution.

Figure 10a shows the general asymmetric structure of the membranes: voidal substructure and a dense region at the fibre wall. This phenomenon is well known in wet spinning of conventional solid fibres[4]. Rapid coagulation of the outer layer results in the formation of a dense structure, which may be oriented, depending on the rheological conditions of the dope as phase change takes place. Once formed, the outer skin and, in this case, inner skin are sufficiently rigid to maintain their shape. Further coagulation takes place by diffusion of coagulant and solvent through the skin. In the context of hollow fibres, since the solidification process occurs from the lumen and from the coagulation bath, the two solidification fronts must meet. The outer and inner skins act as the separating layers (active layers) while the voidal substructure provides strength but little resistance to the passage of fluids.

Various void structures can be observed as dope concentration is altered. *Figure 10c*, spun from the dope with the highest polymer concentration, shows the fibre with the least overall voidage fraction, yet this membrane seems to have larger voids than the fibre spun from the more dilute polymer solution shown in *Figure 10b*. *Figure 10a*, displaying the 20 wt% spun polysulfone fibre, shows a clear macrovoidal region that coexists with a homogeneous spongy void structure. The electron micrographs indicate that thickness of active layer increases with increasing dope concentration. *Figure 10d* shows the morphology of the PAN copolymer hollow fibres, spun from 25 wt% dope.

No surface pores could be observed in the skins of any of the fibres, even at magnifications of $\times 10000$. This indicates that the diameter of any surface pores was less than 200 Å.

Tensile properties

As with morphology, tensile properties were found to be insensitive to dope extrusion rate and jet stretch ratio.

Table 2 Effect of dope concentration on tensile properties[a]—polysulfone fibres

Dope concentration (wt%)	Tenacity (N/tex)	M_1 (N/tex)	M_2 (N/tex)
20	0.02655 ± 0.0023	0.8008 ± 0.072	0.01528 ± 0.0043
30	0.03070 ± 0.0021	1.030 ± 0.043	0.01053 ± 0.0019
40	0.03249 ± 0.0012	1.143 ± 0.062	0.00912 ± 0.0030

[a] ±95% confidence limits (over at least six tests)

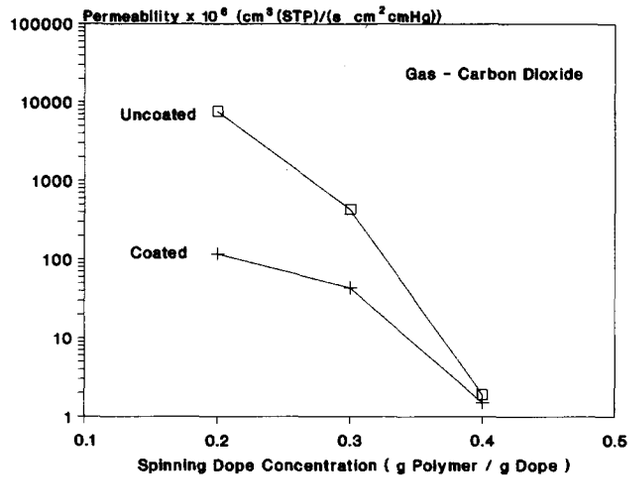

Figure 11 Effect of dope concentration on permeability of polysulfone fibres

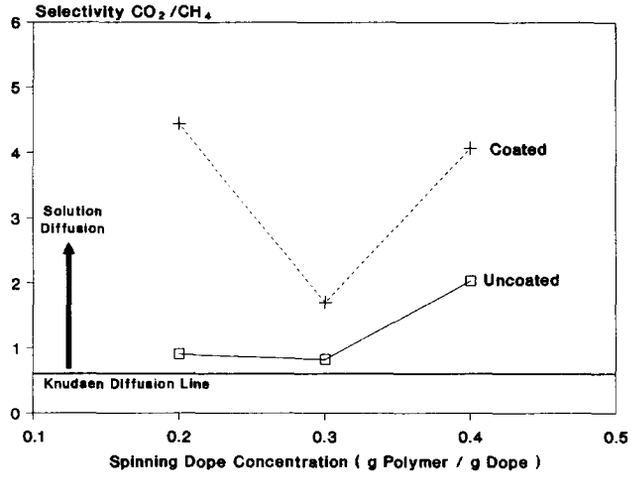

Figure 12 Effect of dope concentration on selectivity of polysulfone fibres

The effect of dope concentration on tenacity, first modulus and second modulus is shown in *Table 2*. Tenacity, which is a measure of the strength of the solid polymer within a fibre, increases with increasing C_D. However, the two moduli are more indicative of polymer structure since they do not depend on conditions of failure, which can be dependent on flaws.

M_1, the resistance of the polymer to elongation before yield, i.e. stiffness, increases with increasing C_D. This may be due to increased cohesion between polymer molecules as they become more densely packed on solidification and/or to greater orientation in the inner skin owing to increased non-Newtonian properties of the polymer solution at higher concentration. However, the structure formed from the more concentrated solutions is in fact less able to resist further elongation after yield, showing a decrease in second modulus, M_2, with increasing dope concentration.

Gas permeation properties

Spinning-dope concentration. *Figures 11* and *12* show the effect of polymer concentration in the spinning dope. Permeability was found to decrease with increasing dope concentration. Coating obviously reduces permeability, and the effect is more marked with fibres spun at low dope concentration. Before coating, the 20 wt% and 30 wt% spun polysulfone fibres exhibited poor selectivities, those associated with Knudsen diffusion through pores in the active layer, i.e. $\Omega_j^i = (MW_j/MW_i)^{1/2} = 0.603$, where MW_j is the molecular weight of species j. The uncoated 40 wt% spun membranes did show solution diffusion properties achieving selectivities of over 2 in favour of CO_2 over CH_4. After coating, the fibres from all three dope concentrations exhibited solution diffusion selectivities. The 20 wt% and 40 wt% spun fibres showed values between 4 and 5, but the selectivities of the 30 wt% fibres were poor, barely reaching 2.

Since the effect of coating is to block surface pores, the large drop in permeability, on coating, of the fibres spun from the least concentrated polymer solution shows that these fibres contain a relatively large surface area of pores. The small drop in permeability, on coating, of the fibres spun from the most concentrated polymer solution indicates that there is a much lower surface area of pores present. It seems likely, therefore, that total surface pore area decreases with increasing spinning-dope concentration.

The effect of coating is to increase selectivity. However, the effect is least with the fibres spun from the intermediate dope concentration of 30 wt%. This can be explained by considering thickness of active layer in the membrane. The electron micrographs indicated that thickness of active layer increases with increasing dope concentration. If the 30 wt% spun fibres have both a relatively thick active layer and large surface area of pores, this would result in the poor coated selectivities of these membranes in comparison to those spun from the other two dope concentrations.

Dope extrusion rate and jet stretch. *Tables 3* and *4* show the influence of dope extrusion rate and jet stretch on hollow-fibre permeability and selectivity. Gas permeation performance is sensitive to the slightest alterations in the character of surface pores. The delicate nature of the membrane surface also results in susceptibility to random pinholes or imperfections. Thus subtle alterations in process conditions, practical procedures or handling in spinning, washing, drying, potting-up, coating or gas permeation testing inevitably cause variations in the separation performance of the hollow fibres. As a result, a distinction has been made between spinning runs in order to confirm the direction of the trends involved.

The effect of dope extrusion rate on gas permeation performance provided the most interesting results of this work. *Table 3* shows that permeability and selectivity increase with increasing dope extrusion rate once the fibres have been coated. Surface pore area increasing with increasing DER would account for the rise in permeabil-

Table 3 Effect of dope extrusion rate on gas permeation properties[a]—polysulfone membranes (PSF 40 wt%)

	Run 1	Run 2	Run 3
DER ($cm^3\ min^{-1}$)	0.7 → 1.0	1.0 → 1.5	1.5 → 2.0
Uncoated *P*	0.0097 → 0.0140	0.0161 → 0.0383	0.0141 → 0.0605
Coated *P*	0.0077 → 0.0172	0.0121 → 0.0244	0.0094 → 0.0144
Uncoated Ω	3.03 → 1.75	1.82 → 2.23	1.92 → 0.87
Coated Ω	3.50 → 4.65	3.36 → 5.32	3.48 → 4.06

[a]JS = 1 = constant; *P* = CO_2 permeability × 10^4 (cm^3(STP)/s cm^2 cmHg); Ω = selectivity CO_2/CH_4

Table 4 Effect of jet stretch on gas permeation properties[a]—polysulfone membranes (PSF 40 wt%)

	Run 1
JS	0.7 → 1.0 → 1.5
Uncoated *P*	0.0167 → 0.0140 → 0.0352
Coated *P*	0.0156 → 0.0172 → 0.0193
Uncoated Ω	2.42 → 1.75 → 0.90
Coated Ω	5.03 → 4.65 → 3.11

[a]DER = 1 $cm^3\ min^{-1}$ = constant; *P* = CO_2 permeability × 10^4 (cm^3(STP)/s cm^2 cmHg); Ω = selectivity CO_2/CH_4

Table 5 Intrinsic gas permeation properties of polymers[a]

Polymer	$\bar{P}_{CO_2} \times 10^9$	$\bar{P}_{CH_4} \times 10^9$	$\Omega^{CO_2}_{CH_4}$
Polysulfone	0.45[21]	0.016	28[21]
Polyacrylonitrile	0.00018[22]	0.000001[23,24]	180
Dimethyl-silicone	325[25]	95[25]	3.4

[a] $\bar{P}$ is the permeability coefficient (cm^3 (STP) cm/scm^2 cmHg) and Ω is the selectivity

ity. Taking a simple view, the increase in surface pore area would cause a decrease in selectivity for uncoated and coated fibres alike, since the selectivity of the silicone coating is much less than that of polysulfone (*Table 5*). The actual rise in selectivity of the coated membranes with increasing DER can be explained by an increase in the selectivity of the polysulfone polymer itself, which is significant enough to cause an increase in the overall selectivity of the coated membrane even though surface pore area is increased with increasing DER.

The results can be related to the rheological behaviour of the spinning dopes under shear. All dopes exhibited shear-thinning behaviour, suggesting that, as the shear rates in the vicinity of the spinneret wall increase due to increasing DER, the polymer molecules become more aligned. This enhanced orientation, 'frozen' into the skin, may cause an improvement in selectivity of the polymer with increasing DER. This would certainly apply to the inner skin of the hollow fibres where coagulation is instantaneous.

Table 4 shows that permeability increases and selectivity decreases with increasing jet stretch ratio for both uncoated and coated fibres. This suggests that, as jet stretch increases, surface pore area increases. During the coagulation process, as incipient skin formation occurs, elongation of the weak skin will occur. Failure of the thin membrane will take place with a constant exposure of new solution to coagulant until the skin is strong enough to resist deformation. The result is an increase in the area of surface pores in the skin. The effect would be predominant on the inner surface.

POLYACRYLONITRILE COPOLYMER MEMBRANES

Fibres were spun from from 25 wt% PAN copolymer dope—the most concentrated dope that could be produced from this polymer. No correlation involving jet stretch or dope extrusion rate was found. Selectivity was consistently poor—invariably around unity. Even the lowest-permeability fibres, 0.002 × 10^{-4} (cm^3(STP)/s cm^2 cmHg), showed a selectivity of only 0.7 CO_2/CH_4.

PAN copolymer has a high intrinsic selectivity of 180 CO_2/CH_4 compared with 28 for polysulfone. However, PAN copolymer has an extremely low intrinsic permeability, thousands of times less than that of polysulfone (*Table 5*). The low intrinsic permeability of PAN copolymer causes most of the gas to flow through any surface pores/imperfections in such membranes. As a result, PAN copolymer membranes need to have an extremely thin and imperfection-free active layer in order for the high intrinsic selectivity of the polymer to be realized at sufficient permeate fluxes. The wide variation found in the permeabilities of the hollow fibres may be a result of the dependence of the PAN copolymer membranes on random surface imperfections. The fact that the permeability of the PAN copolymer membranes is affected by coating solution strength may be indicative of their high dependence on flow through pores partially filled with silicone rather than diffusion through the solid PAN copolymer itself.

With such inherent properties of the PAN copolymer, it is no surprise that the selectivities were poor. Silicone penetration depth as a fraction of total pore length would appear to be insufficient for the silicone coating to cause a rise in selectivity above unity; the Knudsen diffusion through the remainder of the open pores remaining dominant[17].

REFERENCES

1 van't Hof, J. A., Reuvers, A. J., Boom, R. M., Rolevink, H. H. M. and Smolders, C. A. J. *Membr. Sci.* 1992, **70**, 17
2 East, G. C., McIntyre, J. E., Rogers, V. and Senn, S. C. Proc. 4th BOC Priestly Conf., Royal Society of Chemistry, London, 1986, p. 130
3 Borneman, Z., van't Hof, J. A., Smolders, C. A. and van Veen, H. M. Proc. 4th BOC Priestly Conf., Royal Society of Chemistry, London, 1986, p. 145
4 Ziabicki, A. 'Fundamentals of Fibre Formation', Wiley, New York, 1976
5 Paul, D. R. *J. Appl. Polym. Sci.* 1969, **13**, 817
6 Barakat, N. and Hindeleh, A. M. *Textile Res. J.* 1964, **34**, 581
7 Perepelkin, K. E. and Pugach, B. M. *Khim Volokna* 1974, **1**, 48
8 Aptel, P., Abidine, N., Ivaldi, F. and Lafaille, J. P. *J. Membr. Sci.* 1985, **22**, 199
9 Ferguson, J. and Hudson, N. E. *J. Phys.* (*E*) 1975, **8**, 526
10 Jackson, K. P., Walters, K. and Williams, R. W. *J. Non-Newtonian Fluid Mech.* 1974, **14**, 173

11 Jones, D. M., Walters, K. and Williams, P. R. *Rheol. Acta* 1987, **26**, 20
12 Cabasso, I. 'Encyclopedia of Chemical Technology' (Eds R. E. Kirk and D. F. Othmer), 3rd Edn, Wiley Interscience, New York, 1980, Vol. 12, p. 492
13 Brooks, A. A., Henis, J. M. S., Kurz, J. E., Readling, M. C. and Tripodi, M. K. (Monsanto Co.) GB Patent 2047162A, 1980
14 Espenan, J. M. and Aptel, P. 'Membranes and Membrane Processes'(Eds E. Drioli and M. Nakagaki), Plenum, New York, 1986, p. 151
15 Goff R. A. (Monsanto Co.) US Patent 4493629, 1985
16 Ward, R. R., Chang, R. C., Danos, J. C. and Carden, J. A., Jr (Monsanto Co.) US Patent 4214020, 1980
17 Shilton, S. J. *PhD Thesis*, University of Strathclyde, 1992
18 Lodge, A. S. 'Elastic Liquids' Academic Press, New York, 1964
19 Hudson, N. E., Ferguson, J., Warren, B. C. H. and Subotic, D. Proc. Xth Int. Congress on Rheology, Sydney, 1988, Vol. 1, p. 416
20 McKay, G. R., Ferguson, J. and Hudson, N. E. *J. Non-Newtonian Fluid Mech.* 1978, **4**, 89
21 Chern, R. T., Koros, W. J., Hopfenberg, H. B. and Stannett, V. T. 'Materials Science of Synthetic Membranes' (Ed. D. R. Lloyd), ACS Symp. Ser., 1985, p. 25
22 Allen, S. M., Fujii, M., Stannett, V., Hopfenberg, H. B. and Williams, J. L. *J. Membr. Sci.* 1977, **2**, 153
23 Henis, J. M. S. and Tripodi, M. K. *Sep. Sci. Technol.* 1980, **15** (4), 1059
24 Rogers, C. E., Fels, M. and Li, N. N. 'Recent Developments in Separation Science' (Ed. N. N. Li), CRC Press, Cleveland, OH, 1972, Vol. II, p. 107
25 Robb, W. L. *Ann. NY Acad. Sci.* 1967, **146**, 119